KSCE Journal of Civil Engineering (2018) 22(12):4872-4881
Copyright ⓒ2018 Korean Society of Civil Engineers
DOI 10.1007/s12205-017-1581-y

Geotechnical Engineering

pISSN 1226-7988, eISSN 1976-3808
www.springer.com/12205

Simulating Strength Parameters and Size Effect of Stochastic Jointed Rock Mass using DEM Method

Chong Ma*, Wenmin Yao, Yuan Yao***, and Jun Li******

Received October 12, 2017/Revised 1st: January 24, 2018, 2nd: March 27, 2018/Accepted June 15, 2018/Published Online October 18, 2018

Abstract

The strength parameters and the size effect of stochastic jointed limestone rock mass is investigated in this paper. Based on extensive statistics of joint parameters of rock mass in the research region, the probable distribution of geometric characteristic parameters of discontinuities are obtained by the probability graph method. Then the Monte-Carlo method is used for discontinuities network modeling. In addition, 3DEC software and its built-in FISH programming language are used to establish the stochastic jointed rock mass network model based on discrete element method. Triaxial numerical simulation tests under variable confining pressure are conducted with different model sizes and dip angles of bedding planes. The numerical simulation results indicate that the jointed rock mass exhibits weak anisotropy property and significant size effect when it is cut by stochastic discontinuities; the mechanical strength parameters of rock mass begins to fluctuate distinctly as the model size increases, and tend to be stable once the model size reaches or exceeds 4 m × 4 m × 8 m. Besides, the comprehensive mechanical parameters of rock mass in the research region are determined and failure modes of rock mass are analyzed as well based on the numerical simulation results.

Keywords: *stochastic jointed rock mass, numerical simulation, parameters of rock mass, size effect*

1. Introduction

The values of mechanical strength parameters of jointed rock masses have great influence on the stability and safety of geological bodies and above constructions (Sridevi and Sitharam, 2000; Wang *et al.*, 2013). Due to the anisotropy, inhomogeneity and discontinuity, the mechanical parameters of jointed rock masses exhibit obvious size effect (Harrison *et al*., 2000). In addition, the mechanical behaviors of rock masses are greatly influenced by joint distribution characteristics (Zhang *et al*., 2012; Ivanov*a et al.*, 2014), making it extremely complicated to determine the mechanical parameters of jointed rock masses (He, 2001). There have been many studies on proper determination and the size effect of mechanical parameters of jointed rock masses (Grenon and Hadjigeorgiou, 2012). Existing research methods available for studying the size effect of mechanical parameters of jointed rock masses include experimental method, analytical method and numerical simulation method (Oda, 1988). However, due to the limitation of sample size of laboratory tests, cost requirement and difficulties of the in situ tests, it is difficult to study the Representative Elementary Volume (REV) through experimental method (YAN *et al*., 2009).The analytical method can offer clear expressions and accurate results (Zhou *et al.*, 2007; Yang *et al*., 2011), but also have the shortcomings of complex realization process and low applicability.

Benefiting from rapid development of computer technology, the method of numerical simulation in determining the mechanical parameters of jointed rock masses becomes more and more popular (Robinson, 1983; Kulatilake *et al.*, 2001; Dowd *et al*., 2009). The numerical methods mainly include finite element method (Zhang, 2006; Chen *et al.*, 2008; Xu and Dowd, 2010) and discrete element method (Kulatilake *et al*., 1993; Min, 2004). According to previous researches, Discrete Fracture Network (DFN) modeling is becoming an important means for probing into issues of rock mechanics (Han *et al*., 2016), and many related numerous modeling methods have been developed (Dershowitz *et al*., 2004; Dowd *et al*., 2007). Robinson (1983) studied the seepage in rock fractures by stochastic joint network simulation, which show that the critical density can be estimated from the known lattice results and that the behavior for various probability distribution functions for angle and length can readily be predicted. Hudson *et al.* (1983) made a scrutiny into statistical analysis of the geological parameters of joints, and a systematic statistical method was proposed, which make an essential preparation for the numerical modeling. Wang *et al.* (2011) presented a comprehensive system by combining with empirical method,

*Lecturer, School of Mathematical and Physics, China University of Geosciences, Wuhan 430074, China (E-mail: machong@cug.edu.cn)
**Ph.D. Candidate, Faculty of Engineering, China University of Geosciences, Wuhan 430074, China (Corresponding Author, E-mail: wmyao1992@cug.edu.cn)
***M.Sc. Candidate, Faculty of Engineering, China University of Geosciences, Wuhan 430074, China (E-mail: cugyaoyuan@qq.com)
****M.Sc. Candidate, Faculty of Engineering, China University of Geosciences, Wuhan 430074, China (E-mail: 1004536586@qq.com)

laboratory test and numerical simulation, to determine the mechanical parameters of jointed rock masses. Wang *et al.* (2013) presented an improved processes of the stochastic generation of a discontinuous rock mass model with PFC2D, PFC2D is combined with joint network generationmethod to examine the mechanical behaviors of jointed mass. Xu *et al.* (2015) proposed a new elasto-plastic constitutive model for jointed rock mass, which can consider the persistence ratio in different visual angle and anisotropic increase of plastic strain; Bahaaddini *et al.* (2015) studied the effect of joint geometrical parameters of nonpersistent rock mass on Uniaxial Compressive Strength (UCS) and the deformation modulus studied by using the discrete-element particle flow code PFC3D. Han *et al.* (2016) presented a method for modeling 3D fracture networks in a rock mass and obtained a suitable 3D fracture network model for the rock mass at the Songta dam site. Based on the Monte-Carlo method, Chang (2012) extended the stochastic fracture network modeling function of Universal Distinct Element Code (UDEC) and studied the influence of different factors on slope stability, which included including the geometric parameters of joints, and the mechanical parameters of discontinuities, etc.

According to the above situation, most researches are about the size effect of mechanical parameters and anisotropy of jointed rock masses under two-dimensional conditions, but few achievements are conducted based on the true complex joint distributions under three-dimensional conditions. Meanwhile, anisotropy is rarely considered in studying mechanical parameters of rock masses. An appropriate method is of great significance to accurately estimate the strength parameters of jointed rock masses.

In this paper, stochastic rock mass of a high open-pit slope at Esheng limestone mine in Sichuan of china is illustrated to introduce a procedure to obtain mechanical parameters based on a 3-dimensional simulation numerical method. The size effect and failure modes of stochastic jointed rock mass are also analyzed. This research provides a new method for determining mechanical parameters of stochastic jointed rock mass in engineering via DFN fissure network model and Monte Carlo method based upon field investigation of rock joints.

2. Probability Distribution Function of Stochastic Structural Plane

2.1 Development Characteristics of Stochastic Discontinuities

Esheng open-pit mine is located in Emeishan City, Sichuan Province, China, with the main lithology of limestone. The stratums in this mine belong to Maokou, Liangshan and Qixia Formation of Permian, covered by Quaternary locally. The widely developed discontinuities cut the rock mass and formed unstable blocks, which greatly affect the mechanical properties of rock mass and the slope stability, as shown in Fig. 1. According to the existing reports on engineering geological investigations, the dip direction of bedding plane is 305 ~ 335° (with the mean of 320°) and dip angle ranges from12 to 20° (with the mean of 15°). The discontinuities are divided into three groups as follows: J1: dip direction of 0 ~ 24° (with the mean of 12°) and dip angle between 78 ~ 86° (mean: 81°); J2: dip direction between 120 ~ 155° (mean: 135°) and dip angle between 70 ~ 88° (mean: 82°); J3: dip direction between 90 ~ 128° (mean: 109°) and dip angle between 79~85° (mean: 82°).Since discontinuities have great dip angles, karst corrosion channels are often observed near the shallow fractures, and the fractures are usually filled with Quaternary regolith. The deep fractures are mostly filled with later calcite veins and developed with karst cavities and corrosion zones. Most of the corrosion zones are filled with limestone fragments and clay.

Fig. 1. Discontinuities in Esheng Open-pit Mine

2.2 Probability Analysis of Geometric Characteristic Parameters of Discontinuities

The development of discontinuities in rock masses is stochastic, which means the geometric characteristic parameters (i.e., occurrence, trace length, gap width, and spacing) of discontinuities are stochastic variables with certain statistical regularity and can be described by the corresponding probability distribution model (Priest and Hudson, 1981).

Probability graph method is used to determine the most appropriate probability distribution function, which is a precondition for

Table 1. Probability Statistical Parameter Values of Occurrence of Discontinuities

Group of structural plane	Dip direction (°)					Dip angle (°)				
	Distribution	Mean	SD	Min.	Max.	Distribution	Mean	SD	Min.	Max.
J_0	Uniform	303.5	15.29	260	350	Uniform	15	3.46	10	24
J_1	Normal	13.2	4.8	5	25	Normal	77.8	4.3	70	86
J_2	Normal	130.5	7.5	115	146	Uniform	80	4.3	65	89
J_3	Normal	166.5	10.2	137	178	Normal	76.1	9.5	50	87

Table 2. Probability Statistical Parameter Values of Spacing of Discontinuities

Group of structural plane	Spacing (m)				
	Distribution	Mean	SD	Min.	Max.
J_0	Negative exponent	0.51	0.51	0.1	2.2
J_1	Negative exponent	1.11	1.11	0.1	4
J_2	Negative exponent	1.89	1.89	0.1	4.2
J_3	Negative exponent	1.25	1.25	0.1	3.5

Table 3. Probability Statistical Parameter Values of Trace Length of Discontinuities

Group of structural plane	Trace length (m)				
	Distribution	Mean	SD	Min.	Max.
J_0	Continuous				
J_1	Negative exponent	0.9	0.9	0.13	2.55
J_2	Negative exponent	1.05	1.05	0.13	2.55
J_3	Negative exponent	0.83	0.83	0.25	2.55

Table 4. Probability Distributions of Diameters of Discontinuities

Group of structural plane	Diameter (m)				
	Distribution	Mean	SD	Min.	Max.
J_0	Continuous				
J_1	Negative exponent	1.15	1.15	0.127	2.54
J_2	Negative exponent	1.34	1.34	0.127	2.54
J_3	Negative exponent	1.06	1.06	0.254	2.54

Table 5 Calculated Results of Volume Densities of Discontinuities

Group of structural plane	Linear density (m^{-1})	Mean trace length (m)	Mean diameter (m)	Volume density (m^{-3})
J_0	According to mean spacing			
J_1	0.901	0.9	1.15	0.43372
J_2	0.529	1.05	1.34	0.187554
J_3	0.800	0.83	1.06	0.453271

subsequent establishment of three-dimensional models with stochastic discontinuities. Specifically, with the value of F (calculated by F-test) as the criteria, multiple distribution forms, i.e., normal distribution, uniform distribution, exponential distribution and log-normal distribution are fitting and compared to determine the optimal probability distribution function and relevant parameters.

Based on the measurement of discontinuities in the field, the most suitable probability distribution of different geometric parameters (occurrence, spacing and trace length) of discontinuities for the bedding plane J0 and the other three dominant joint groups J1, J2 and J3 are determined. Types of probability distributions and values of the geometric characteristic parameters of each dominant joint group are listed in Tables 1-3.

3. Numerical Simulation Tests of Stochastic Jointed Rock Mass by Three-dimensional Discrete Element Method

3.1 Establishment of 3D Network Model

The discontinuities are assumed to be thin discs during the numerical simulation, and are determined by their diameters (Kulatilake and Wu, 1986). The assumption of the discontinuities as thin discs is a basic assumption in 3DEC software, as well as UDEC, PFC3D and PFC2D, which are all numerical softwares based on discrete element method. According to Table 3, the diameter based on the probability distributions can be obtained, as shown in Table 4.

The bulk density is one of the key factors of in discontinuity network simulation, which can be obtained by the corresponding relationship with linear density. Linear density was calculated by spacing of discontinuities (Oda, 1988; Wang *et al.*, 2013). The Calculated results of volume densities of different group of structural plane are as shown in Table 5.

A basic assumption in the three-dimensional network simulation is that the discontinuities is discoid and have the same occurrence probability in the study area (Kulatilake and Wu, 1986; Xu and Dowd, 2010). The essential factors for the establishment of 3D network model are the number, attitude, diameter and central position of each discontinuity. The bulk density and the number of the planes of the unit volume structure can be obtained based on the average spacing (Oda, 1988; Min and Jing, 2004). The attitude and diameter of the discontinuities are randomly generated by using Monte-Carlo method according to the probability distribution type and the corresponding characteristic parameters. Furthermore, it is considered that the coordinate of the central coordinate of the discontinuities are distributed uniformly in the model range.

Three-dimensional fracture networks are set up based on Discrete Fracture Network (DFN) model established in software 3DEC.

With the data listed above, a large structural plane network model sized 30 m × 30 m × 30 m was established, as shown in Fig. 2, and the two-dimensional cross sections of different directions

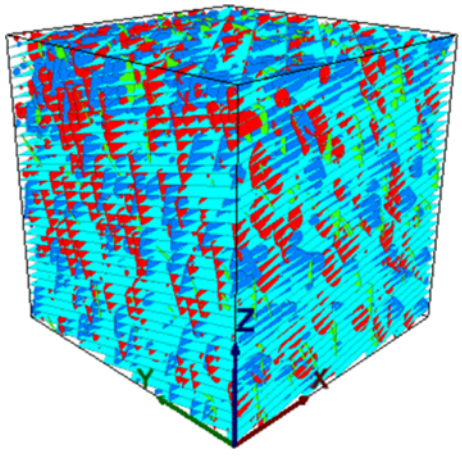

Fig. 2. Three-dimensional Network Model (30 m × 30 m × 30 m) of Discontinuities

are shown in Fig. 3.

3.2 Network Calculation Model for Stochastic Discontinuities

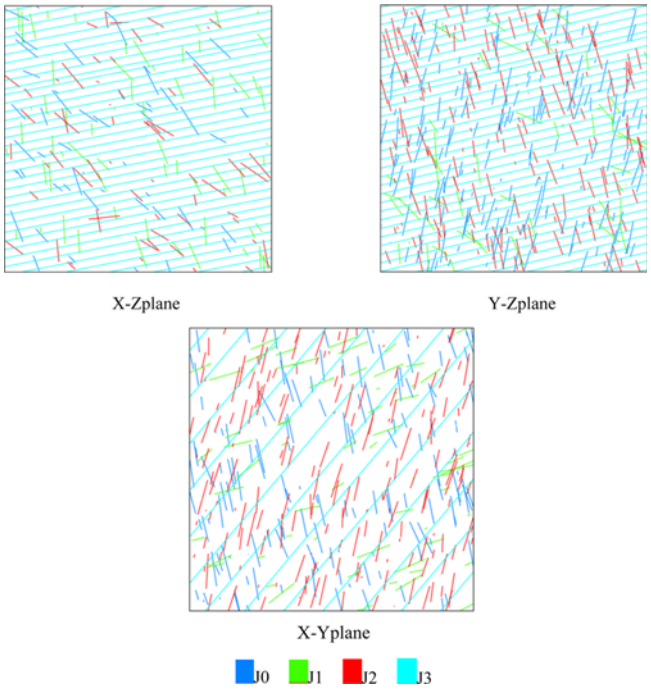

Fig. 3. Two-dimensional Cross Sectionsof Different Directions (30 m × 30 m × 30 m)

Based on the three-dimensional network for stochastic discontinuities shown in Fig. 2, the Discrete Fracture Network (DFN) is established with a mechanical definition to transit the geometric model to the mechanical numerical model, as shown in Fig. 4. In Fig. 4(a), the mechanical parameters at the red nodes are identical to the parameters of rock blocks, while those at the blue nodes in the circle are identical to the mechanical parameters of discontinuities. Then equivalent mechanical simulation of discontinuous discontinuities can be realized. The distribution map of cohesion in the numerical calculation model is shown in Fig. 4(b).

3.3 Numerical Test Scheme

Based on laboratory test, the mechanical parameters of rock and discontinuity are list in Tables 6-7.

In order to investigate the influences of size effect and anisotropy

Table 6. Mechanical Parameters of Rock

Unit weight (kN/m^3)	Young's modulus (GPa)	Poisson's ratio	Uniaxial compressive strength (MPa)	Cohesion (MPa)	Internal friction angle (°)
2680	36.3	0.263	56	10.02	43.5

Table 7. Mechanical Parameters of Discontinuity

Normal stiffness (GPa/m)	Shear stiffness (GPa/m)	Cohesion (MPa)	Internal friction angle Z(°)
250	50	0	24.3

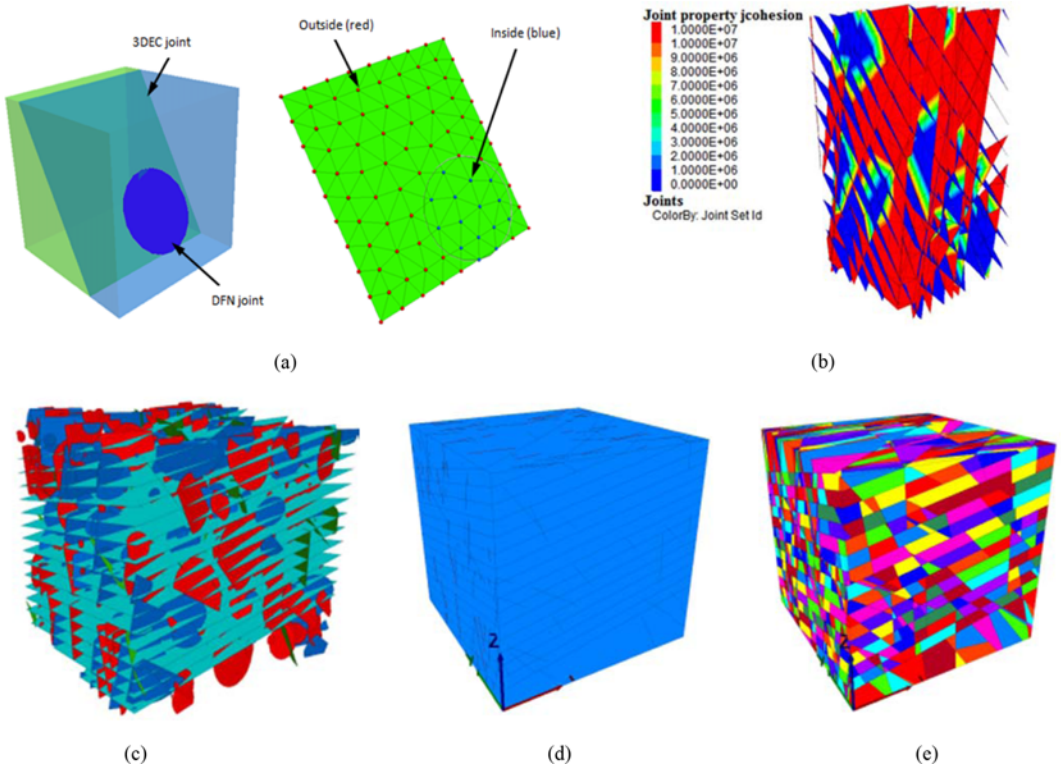

Fig. 4. Realization of Calculation Network for Stochastic Discontinuities: (a) Mechanical Definition of DFN joint, (b) Cohesion Distribution Map, (c) DFN, (d) Three-dimensional Network Model for Discontinuities, (e) Three-dimensional Network Calculation Model

on the strength parameters of rock mass, the following sizes of triaxial numerical test models are: 0.5 m × 0.5 m × 1 m, 1 m × 1 m × 2 m, 2 m × 2 m × 4 m, 4 m × 4 m × 8 m, 6 m × 6 m × 12 m.The sizes are chosen based on the network calculation model for stochastic discontinuities. Meanwhile, considering the anisotropy of rock mass, the dip angle β of bedding planes was 0°, 15°, 24°, 45°, 60° and 90°, respectively.

The confining pressure is obtained by calculating the gravity of the overlying rock mass in the sampling site. The height and the density of the overlying rock mass are two main parameters. In this research, the height of overlying strata of the samples in the field is about 18 m, and the density of the rock mass is 3150 kg/m^3. In this way, the maximum confining pressure is chosen to be 6 MPa, and other values are chosen as 1 MPa, 2 MPa, 4 MPa and 6 MPa, respectively.

Triaxial numerical tests are conducted to obtain the stress-strain curves of model samples under the confining pressure of 1 MPa, 2 MPa, 4 MPa and 6 MPa respectively. Each loading process is-recorded. Finally, the test data is analyzed to get the values of maximum principal stress and strength parameters when sample failure occurs.

In the numerical test, the Mohr-coulomb constitutive relationship

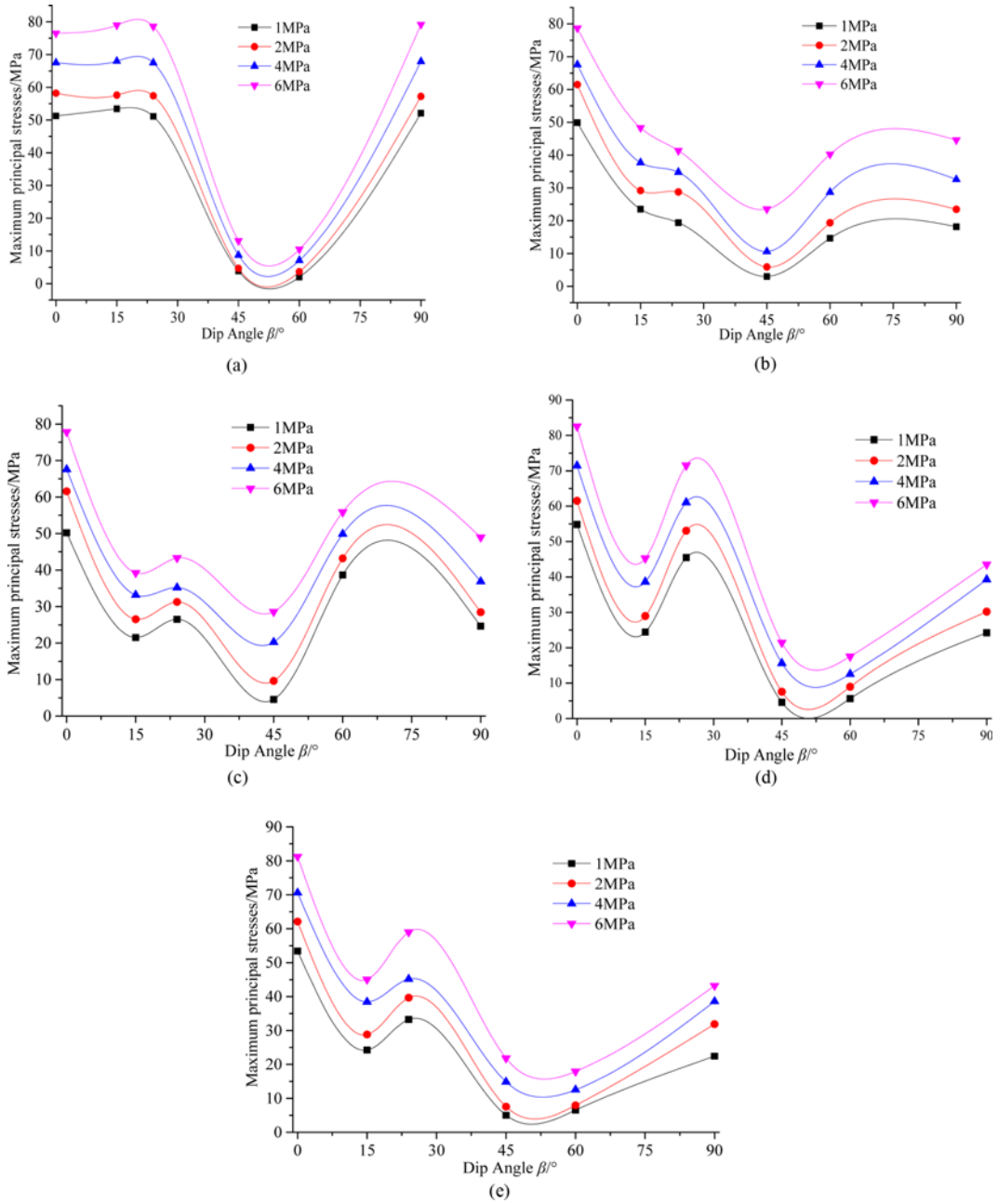

Fig. 5. The Variation Trends of the Maximum Principal Stress with the Dip Angle β: (a) Model Size: 0.5 m × 0.5 m × 1 m, (b) Model Size: 1 m × 1 m × 2 m, (c) Model Size: 2 m × 2 m × 4 m, (d) Model Size: 4 m × 4 m × 8 m, (e) Model size: 6 m × 6 m × 12 m

is adopted, which is one of the most commonly used constitutive models in geotechnical engineering, and engineering geology.

Considering that the samples of the tests are cylinders and the pressure is applied on the faces of the samples, we define the top and bottom faces of the samples as the axial boundaries and the lateral faces as the lateral boundaries. According to precious research (Bahaaddini *et al*., 2015; Wang *et al.*, 2013), lateral boundary of the model is set as free constraint, and the axial boundary is set as fixed constraint. When triaxial test with equal confining pressure is conducted, the confining pressure is applied on the lateral boundary and the top firstly until the model is balanced. The confining pressure is determined by the field stress state of the rock mass. Then displacement with a constant displacement rate (0.047 mm/s) is applied on top of the model until the rock mass is damaged, during which the axial pressure will be monitored.

4. Numerical Test Results

4.1 The Effect of Anisotropy on the Maximum Principal Stress

After the numerical calculation, the maximum principal stresses. The maximum principal stresses, the maximum value of the axial stress during the numerical tests, which are obtained from the stress-strain curves under different model sizes and dip angles of discontinuities.

Figure 5 shows the variation trends of the maximum principal stress with the dip angle of discontinuities under different model sizes.

The following conclusions can be drawn through analysis of Fig. 5: (1) when the model size is fixed, the maximum principal stress of the model increases as the confining pressure increases. (2) When the model size changes, the curve change trend varies. But the curve demonstrates the same trend after the model size is increased to 4 m × 4 m × 8 m or further.

4.2 The Effect of Anisotropy on the Strength Parameters

Strength parameters mainly include cohesion and internal friction angle of the rock mass. To analyze the effect of anisotropy on the strength parameters, the variation trends of cohesion and internal friction angle values with the dip angle of discontinuities are plotted as shown in Fig. 6 and Fig. 7.

According to Fig. 6, the range of cohesion in stochastic fractured jointed rock mass is 0 ~ 10 MPa, which is between the cohesion of discontinuities and rock blocks. Meanwhile, the range of internal friction angle change in stochastic fractured jointed rock mass is 24° ~ 43°, which is mostly between the internal friction angle of discontinuities and rock blocks, as shown in Fig. 7. As the dip angle β of discontinuities increases, the trend of cohesion and internal friction angle both exhibits the law of "decrease-increase-decrease-increase" in general. As can be seen from analysis of the range of cohesion and internal friction angle under different dip angles β when the model size is fixed, the difference between the maximum and minimum values of cohesion can reach 90% ~ 100%, while difference between internal friction angle is nearly 50%. So, we can conclude that the cohesion is more sensitive to the effect of anisotropy of rock mass than the internal friction angle.

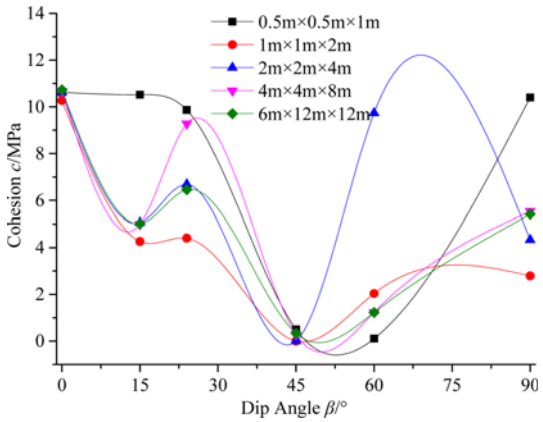

Fig. 6. Variation Trend of Cohesion with the Dip Angle

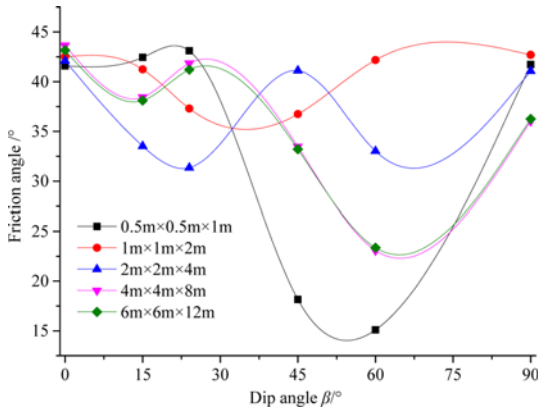

Fig. 7. Variation Trend of Internal Friction Angle with the Dip Angle

4.3 Effect of Model Size on Strength Parameters

To analyze the size effect of strength parameters and determine the Representative Elementary Volume (REV) of jointed rock mass, variation trends of cohesion and internal friction angle with the model size under the same dip angle of discontinuities are plotted in Fig. 8 and Fig. 9, respectively.

According to Fig. 8 and Fig. 9, as the model size increase, the cohesion and internal friction angle present the same trends. With the model size increasing, strength parameters are unstable until the model size reaches 4 m × 4 m × 8 m. After the model size is increased to 4 m × 4 m × 8 m, it can be observed that the amplitude of variation of strength parameters reduces significantly, which further suggests that the strength parameters of this rock mass structure has an obvious size effect and the REV of rock mass in the research area is about 4 m × 4 m × 8 m.

The mechanism of strength loss of rock mass is influenced by many factors, and remains a challenge for us even in today. Here, we mainly discuss the mechanical parameters of the jointed rock

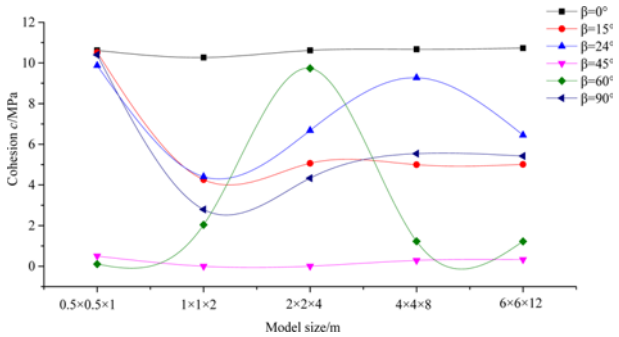

Fig. 8. Variation Trend of Cohesion with the Model Size

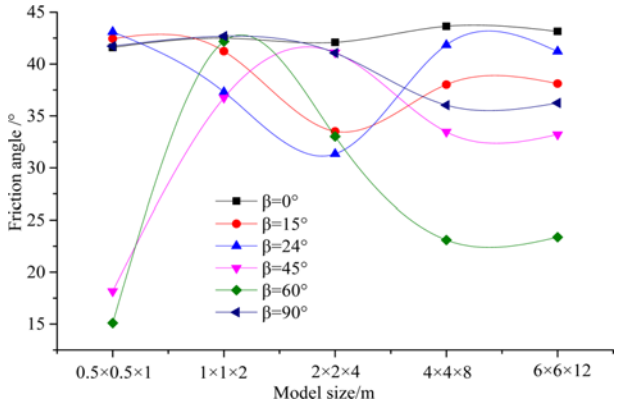

Fig. 9. Variation Trend of Internal Friction Angle with the Model Size

mass. The mechanism which leads to the complicated behaviors of rock mass will be discussed in the further study.

5. Comparisons of DEM with Traditional Methods

The average attitude of bedding planes in the research area is about 320° ∠ 15°. According to the engineering geological conditions, there is no tectonic stress in the research area; therefore, the maximum principal stress of rock mass comes from the gravity of overlying rock. The strength parameters calculated by numerical calculation can be considered to be equal to the actual strength parameters of rock mass, when the dip angle β of discontinuities is 15°. Taking into account the size effect, the REV is about 4 m × 4 m × 8 m, which means the mechanical parameters remain stable when the size of model reaches of exceeds 4 m × 4 m × 8 m, so the results of numerical calculation are taken as the values of mechanical parameters of rock mass when the model size is 6 m × 6 m × 12 m.

For the purpose of comparative analysis, the RMR (Rock Mass Rating) and GSI (Geological Strength Index) scoring systems based on Hoek-Brown criterion are used for empirical estimation of the strength parameters of rock mass.

Table 9. Strength Parameters of Rock Mass Obtained by Amended Hoek-Brown Criteria

GSI	σ_c (MPa)	m_i	D	c_m (MPa)	φ_m (°)
83	53	12	0.5	4.821	39.83
72	53	12	0.5	3.545	35.72
60	53	12	0.5	2.741	31.03

Table 10. Comparative Analysis of Three Methods

Strength parameter	Distinct element method	*RMR* scoring method	*GSI* scoring method
C (MPa)	5.012	1.447	2.741
φ (°)	38.11	26.237	31.02

The value of RMR should be determined firstly when using RMR scoring systems, which are on the base of the structure characteristics of rock mass, statistical results of field structural surface measurement and the uniaxial compressive strength of rock. The value of RMR is listed in Table 8. Then the value of m_i, the coefficient of strength characteristics, is determined by the lithology description of rock mass. The strength parameters of rock mass can be obtained according to the approach introduced by Hoek and Brow (1997) and listed in Table 10.

When using the GSI scoring systems, there are four basic parameters should be determined. First, the value of m_i, c_m (Uniaxial compressive strength) are determined by the same way as the RMR. Then GSI and D (coefficient of disturbance) are determined based on the characteristic of rock mass structure and discontinuities. Finally, amended Hoek- Brow criterion is used to obtain the strength parameters as shown in Table 9.

Table 10 shows the strength parameters obtained by three methods. As can be seen from Table 10, the distinct element method gives the maximum strength parameters of rock mass, followed by the *GSI* and *RMR* scoring systems in sequence. The *RMR* and *GSI* scoring systems use similar principles and forms of calculation formula. The main difference between *RMR* and *GSI* is the grading of the rock masses. The *GSI* scoring system focuses on lithology, structure of rock mass, crushing degree of rock mass and surface characteristics of discontinuities, which means this method is very subjective and can be great difference when rated by different persons (HOEK, 1992); therefore, it is often very difficult to describe the surface characteristics of discontinuities accurately. Meanwhile the *RMR* scoring system

Table 8. Value of *RMR*

Weathering	Rock strength		RQD		Spacing of joint		Joint state	Ground water		Total
	Strength (MPa)	Score	RQD (%)	Score	Spacing (cm)	Score	Score	Description	Score	
Weak	53	7	42	8	42	10	25	Moisture	7	57

classifies *RMR* values into five ratings which are given different meanings to evaluate the quality of rock mass [Hoek and Brow, 1997]. This method reduces the influence of subjectivity to some extent and also strictly controls *RMR* values within an upper limit. As for the Discrete Element Numerical method, the mechanical parameters are determined mainly from the mechanical perspective and obtained according to the total stress-strain curves when failure of rock mass occurs based on three-dimensional numerical simulation tests. This method basically eliminates the influence of subjectivity, and can providing more reliable results.

6. Failure Modes of Stochastic Jointed Rock Mass

A number of factors can affect the failure modes of rock mass, mainly including dip angle β of bedding planes, confining pressure, model size, etc. But as for stochastic jointed rock mass, the size may determine its failure mode. The possible failure modes of small and large-size rock masses are discussed respectively through displacement contour map, velocity contour map and vectograms of the numerical calculation results in the following subsections.

6.1 Failure Modes of Small-size Rock Mass

For small model sizes, the failure modes of rock mass can be classified into multiple sliding failure mode and combined

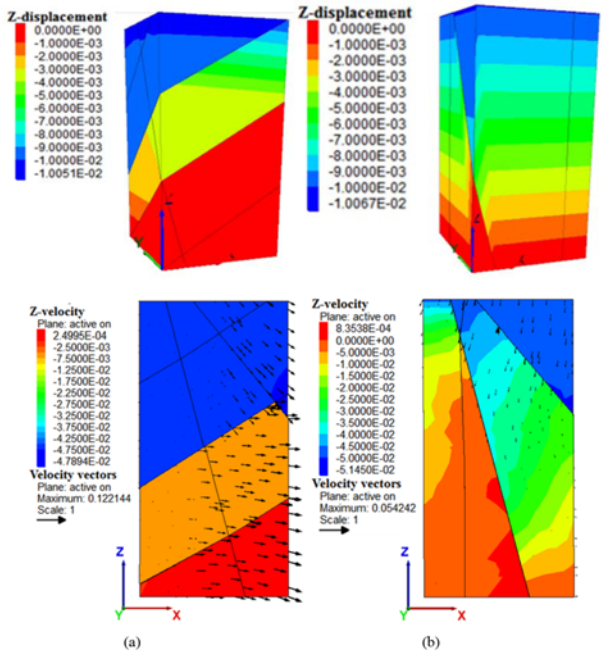

Note: Multiple sliding failure mode means sliding failure along multiple discontinuities; Combined failure mode means that both discontinuities and rock blocks are subject to failure.

Fig. 10. Typical Failure Modes of Small-size Models: (a) Multiple Sliding Failure Mode, (b) Combined Failure Mode

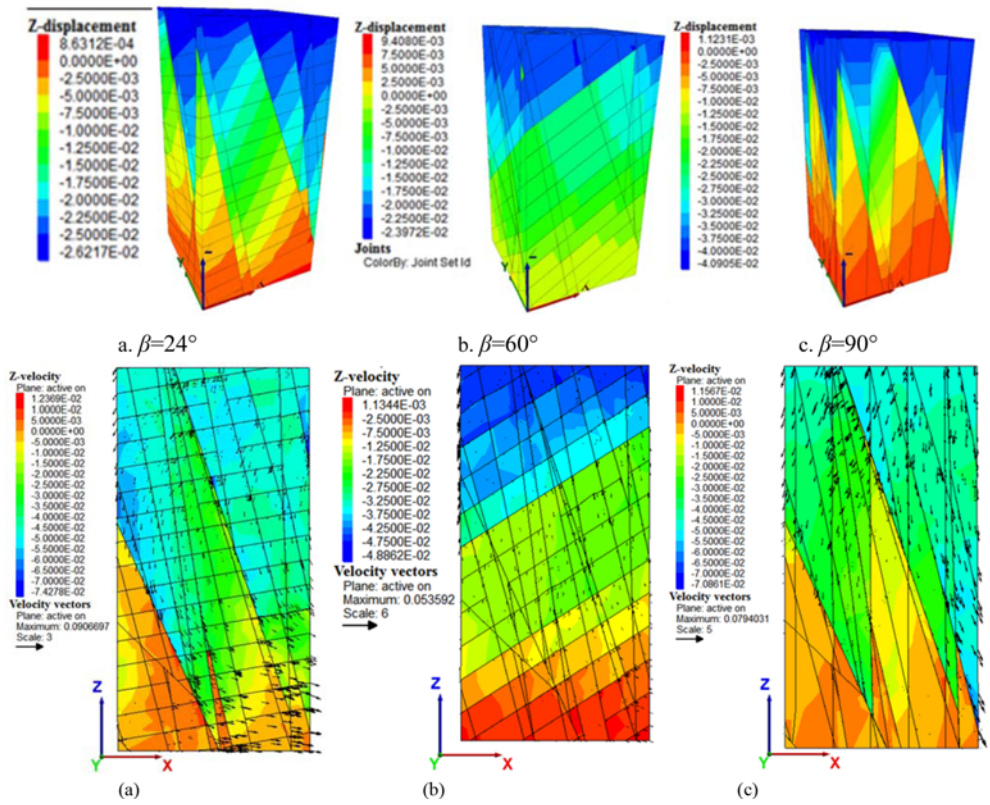

Note: Multiple sliding failure mode means sliding failure along multiple discontinuities; Combined failure mode means that both discontinuities and rock blocks are subject to failure; Sliding failure mode means sliding failure along the structural plane.

Fig. 11. Typical Failure Modes of Large-size Models: (a) Combined Failure Mode, (b) Sliding Failure Mode, (c) Multiple Sliding Failure Mode

failure mode, as shown in Fig. 10.

As can be seen from Fig. 10: when the dip angle of bedding planes is $\beta = 24°$ and the confining pressure is low, it can be seen that the rock blocks in the rock mass will not be subject to failure through analysis of velocity contours and vectograms in Fig. 10(a). The rock mass has sliding failure along the combined surface of discontinuities. when the dip angle of bedding planes is $\beta = 90°$ or the confining pressure is high, obvious velocity boundaries can be observed from velocity contours and vectograms in Fig. 10(b),which suggests that certain tensile failure and shear failure zones appear in the rock blocks and local sliding or pulling are produced on the structural plane. The failure mode of rock mass is combined by the sliding failure long discontinuities and the failure of the rock block. Under these circumstances, the strength of rock mass is between the strength of discontinuities and rock blocks.

6.2 Failure Modes of Large-size Rock Mass

For large size of model, the failure of rock mass can be classified into three modes as shown in Fig. 11, which are combined failure mode, sliding failure mode and multiple sliding failure mode.

According to Fig. 11, (1) when β is within the range of [0°, 24°] and the rock mass is under high confining pressure, the most possible failure mode of rock mass is combined failure mode. Under such conditions, local tensile or shear failure of rock blocks often occurs, and discontinuities in the rock mass slide or are pulled open, the strength of rock mass is decided by both discontinuities and rock blocks. (2) When β changes within the range of (24°, 60°), it is most possibly that the rock mass is subject to sliding failure which mainly occurs on the bedding planes. In this situation, failure of rock blocks inside rock mass will not generate. The failure of rock mass is sliding failure along the combined discontinuities, and the strength of rock mass is relatively low. (3) When β is within the range of [60°, 90°] and the model is under medium or low confining pressure, the most possible failure mode of rock mass is multiple sliding failure mode. Under this circumstance, failure of rock blocks will hardly occur in the rock mass, and the failure of rock mass will occur along the combined path of its internal discontinuities.

7. Conclusions

In this paper, a systematic study on the characteristics of jointed rock mass strength parameters is conducted. Based on the field investigation and data collection from Esheng limestone open-pit mine, the anisotropy and size effect of jointed rock mass are investigated by using the 3Dsimulationtests and experience estimation method. The results of the research are summarized as follows:

1. Based on field geological investigation, statistical analysis of discontinuities is conducted. The probability distributions of the geometric characteristic parameters of discontinuities are obtained using the probability graph method. The results reveals that for most discontinuities, the dip direction and dip angle have normal distribution, while few discontinuities are uniformly distributed; the spacing and the half-length of the discontinuities are consistent with the negative exponential distribution.
2. Based on the probability distribution models, Monte Carlo method and Fish programming language are applied to the establishment of 3D stochastic joint network model in 3DEC software. With the combination of DFN fissure network model and Monte Carlo method, the numerical tests could well simulate strength properties of the rock mass.
3. Research on the anisotropy and size effect of rock mass strength parameters indicate that the size effect of stochastic joint rock mass would be more obvious, but the impacts of anisotropy would lessen while the rock mass is cut by stochastic discontinuities. According to the numerical simulation test results, the Representative Elementary Volume (*REV*) size of the study area is determined to be 4 m × 4 m × 8 m. Then the joint strength parameters are obtained. Strength parameters obtained by numerical simulation are more reasonable via the comparison to RMR rating system and GSI rating system.
4. Based on the velocity contours and vectograms of numerical simulation, small size rock mass have two failure modes: multiple sliding failure mode and combined failure mode; while there are three failure modes for large size rock mass: multiple sliding failure mode and combined failure mode. Failure modes at specific sizes are related to dip angle β of bedding planes and confining pressure.

Acknowledgements

This research is partially supported by Natural Science Foundation of Hubei Province (CN) (2018CFB385).

References

Bahaaddini, M., Hagan, P., Mitra, R., and Hebblewhite, B. K. (2015). "Numerical study of the mechanical behavior of nonpersistent jointed rock masses." *International Journal of Geomechanics,* Vol. 16, No. 1, p. 04015035, DOI: 10.1061/(asce)gm.1943-5622.0000510.

Chang, J. L. (2012). *Parameter analysis based on random fractured rock slope stability*, M.Sc. Dissertation, Harbin Institute of Technology, Harbin, China.

Chen, S. H., Feng, X. M., and ISAM, S. (2008). "Numerical estimation of REV and permeability tensor for fractured rock masses by composite element method." *International Journal for Numerical and Analytical Methods in Geomechanics*, Vol. 32, No. 12, pp. 1459-1477, DOI: 10.1002/nag.679.

Dershowitz, W. S., La Pointe, P. R., Doe, T. W., and Goslder, A. (2004). "Advances in discrete fracture network modeling." *Proceedings of the US EPA/NGWA fractured rock conference*, Portland, ME, pp. 882-894.

Dowd, P. A., Martin, J. A., Xu, C., Fowell, R. J., and Mardia, K.V. (2009). "A three-dimensional fracture network data set for a block of granite." *International Journal of Rock Mechanics and Mining Sciences*, Vol. 46, No. 5, pp. 811-818, DOI: 10.1016/j.ijrmms.2009.

02.001.

Dowd, P. A., Xu, C., Mardia, K. V., and Fowell, R. J. (2007). "A comparison of methods for the stochastic simulation of rock fractures." *Mathematical Geology*, Vol. 39, No. 7, pp. 697-714, DOI: 10.1007/s11004-007-9116-6.

Du, P. Z., Liu, J., Han, Z. Q., and Xu, H. (2003). "Stability analysis of high rock slope based on meticulous description of complex structure." *Rock and Soil Mechanics*, Vol. 34, No. s1, pp. 393-398, DOI: 10.16285/j.rsm.2013.s1.017.

Grenon, M. and Hadjigeorgiou, J. (2012). "Applications of fracture system models (FSM) in mining and civil rock engineering design." *International Journal of Mining Reclamation and Environment*, Vol. 26, No. 1, pp. 55-73, DOI: 10.1080/17480930.2011.639190.

Han, X., Chen, J., Wang, Q., Li, Y. Y., Zhang, W., and Yu, T. W. (2016). "A 3D Fracture network model for the undisturbed rock mass at the songta dam site based on small samples." *Rock Mechanics and Rock Engineering*, Vol. 49, No. 2, pp. 611-619, DOI: 10.1007/s00603-015-0747-5.

Harrison, J. P., Hudson, J. A., and Popescu, M. E. (2002). "Engineering rock mechanics: Part 2. Illustrative worked examples." *Applied Mechanics Reviews*, Vol. 55, No. 2, pp. B30-B31, DOI: 10.1115/1.1451166.

He, M., Xue, T., and Peng, Y. (2001). "A new way of determining mechanical parameters of engineering rock masses." *Chinese Journal of Rock Mechanics and Engineering*, Vol. 20, No. 2, pp. 225-229, DOI: 10.3321/j.issn:1000-6915.2001.02.017.

Hoek, E. (1994). "Strength of rock and rock mass." *International Society for Rock Mechanics News Journal*, Vol. 2, No. 2, pp. 4-16.

Hoek, E. and Brown, E. T. (1997). "Practical estimates of rock mass strength." *International Journal of Rock Mechanics and Mining Sciences*, Vol. 34, No. 8, pp. 1165-1186, DOI: 10.1016/s0148-9062(97)00305-7.

Hudson, J. A. and Priest, S. D. (1983). "Discontinuity frequency in rock masses." *International Journal of Rock Mechanics & Mining Sciences & Geomechanics Abstracts*, Vol. 20, No. 2, pp. 73-89, DOI: 10.1016/0148-9062(83)90968-3.

Ivanova, V. M., Sousa, R., Murrihy, B., and Einstein, H. H. (2014). "Mathematical algorithm development and parametric studies with the GEOFRAC three-dimensional stochastic model of natural rock fracture systems." *Computers and Geosciences*, Vol. 67, No. 3, pp. 100-109, DOI: 10.1016/j.cageo.2013.12.004.

Kulatilake, P., Malama, B., and Wang, J. (2001). "Physical and particle flow modeling of jointed rock block behavior under uniaxial loading." *International Journal of Rock Mechanics and Mining Sciences*, Vol. 38, No. 5, pp. 641-657, DOI: 10.1016/s1365-1609(01)00025-9.

Kulatilake, P., Wang, S., and Stephansson, O. (1993). "Effect of finite size joints on the deformability of jointed rock in three dimensions." *International Journal of Rock Mechanics and Mining Sciences and Geomechanics Abstracts*, Vol. 30, No. 5, pp. 479-501, DOI: 10.1016/0148-9062(93)92216-d.

Kulatilake, P. and Wu, T. (1986). "Relation between discontinuity size and trace length." *Symposium on Rock Mechanics*, Vol. 27, pp. 130-133.

Min, K. B. and Jing, L. (2004). "Stress dependent mechanical properties and bounds of Poisson's ratio for fractured rock masses investigated by a DFN-DEM technique." *International Journal of Rock Mechanics and Mining Sciences*, Vol. 41, No. 3, pp. 431-432, DOI: 10.1016/j.ijrmms.2003.12.072.

Oda, M. (1988) "A method for evaluating the representative elementary volume based on joint survey of rock masses." *Canadian Geotechnical Journal*, Vol. 25, No. 3, pp. 440-447, DOI: 10.1139/t88-049.

Priest, S. D. and Hudson, J. A. (1981). "Estimation of discontinuity spacing and trace length using scan line survey." *International Journal of Rock Mechanics and Mining Sciences and Geomechanics Abstracts*, Vol. 18, No. 3, pp. 183-197, DOI: 10.1016/0148-9062 (81)90973-6.

Robinson, P. C. (1983). "Connectivity of fracture systems—a percolation theory approach." *Journal of Physics A: Mathematical and General*, Vol. 16, No. 3, pp. 605-614, DOI: 10.1088/0305-4470/16/3/020.

Sridevi, J. and Sitharam, T. G. (2000). "Analysis of strength and moduli of jointed rocks." *Geotechnical and Geological Engineering*, Vol. 18, pp. 3-21, DOI: 10.1023/A:1008992621515.

Wang, P. T., Yang, T. H., Yu, Q. L., Liu, H. L., and Zhang, P. H. (2013). "Characterization on jointed rock masses based on PFC2D." *Frontiers of Structural and Civil Engineering*, Vol. 7, No. 1, pp. 32-38, DOI: 10.1007/s11709-013-0187-9.

Wang, X., Zhao, Y., and Lin, X. (2011). "Determination of mechanical parameters for jointed rock masses." *Journal of Rock Mechanics and Geotechnical Engineering*, Vol. 3, No. Supp., pp. 398-406, DOI: 10.3724/SP.J.1235.2011.00398.

Xu, C. and Dowd, P. (2010). "A new computer code for discrete fracture network modeling." *Computers and Geosciences*, Vol. 36, No. 3, pp. 292-301, DOI: 10.1016/j.cageo.2009.05.012.

Xu, Q., Chen, J., Li, J., Zhao, C., and Yuan, C. (2015). "Study on the constitutive model for jointed rock mass." *PloS One*, Vol. 10, No. 4, p. e0121850, DOI: 10.1371/journal.pone.0121850.

Yan, C. G., Wu, F. Q., Qi, S. W., Liu, T., and Masakatsu, M. (2009). "Deformation and strength parameters and size effect of random jointed rock mass by numerical simulation." *Chinese Journal of Geotechnical Engineering*, Vol. 31, No. 6, pp. 879-885, DOI: 10.3321/j.issn:1000-4548.2009.06.010.

Yang, J. P., Chen, W. Z., and Dai, Y. H. (2011). "Study of scale effect of deformation modulus for fractured rock mass—part II: Analytical method." *Rock and Soil Mechanics*, Vol. 32, No. 6, pp. 1607-1612, DOI: 10.3969/j.issn.1000-7598.2011.06.002.

Zhang, Y. H. (2006). *Research on the equivalent hydro-mechanical parameters of rock mass*, Ph.D. Dissertation, *China University of Geosciences*, Wuhan, China.

Zhang, W., Chen, J. P., Liu, C., Huang, R., Li, M., and Zhang, Y. (2012). "Determination of geometrical and structural representative volume elements at the Baihetan dam site." *Rock Mechanics and Rock Engineering*, Vol. 45, No. 3, pp. 409-419, DOI: 10.1007/s00603-011-0191-0.

Zhou, C. B., Chen, Y. F., and Jiang, Q. H. (2007). "Representative elementary volume and mechanical parameters of fractured rock masses." *Chinese Journal of Geotechnical Engineering*, Vol. 29, No. 8, pp. 1135-1142, DOI: 10.3321/j.issn:1000-4548.2007.08.004.